

***TWITCH*— A MODEL FOR TRANSIENT DIFFUSION, ELECTROMIGRATION, AND CHEMICAL REACTION IN ONE DIMENSION**

VERSION 1.0

Prepared for

**Nuclear Regulatory Commission
Contract NRC-02-88-005**

Prepared by

**Center for Nuclear Waste Regulatory Analyses
San Antonio, Texas**

August 1992



Property of
CNWRA Library

CNWRA 92-019

***TWITCH* — A MODEL FOR TRANSIENT
DIFFUSION, ELECTROMIGRATION, AND
CHEMICAL REACTION IN ONE
DIMENSION**

Prepared for

**Nuclear Regulatory Commission
Contract NRC-02-88-005**

Prepared by

**John C. Walton
Stephen K. Kalandros**

**Center for Nuclear Waste Regulatory Analyses
San Antonio, Texas**

August 1992

CONTENTS

Section	Page
LIST OF FIGURES	iii
LIST OF TABLES	iv
ACKNOWLEDGEMENTS	v
DISCLAIMER	v
1 INTRODUCTION	1-1
2 THEORY	2-1
3 IMPLEMENTATION OF THEORY	3-1
3.1 CORROSION AND CALCULATION OF CURRENT IN SOLUTION	3-2
3.2 POTENTIAL GRADIENT ESTIMATION	3-3
3.3 CALCULATION OF FLUX AND MASS TRANSPORT	3-3
3.4 EQUILIBRATION	3-4
3.5 ERROR CORRECTION THROUGH ELECTRONEUTRALITY	3-5
4 CODE VERIFICATION AND MODEL VALIDATION	4-1
4.1 ALAVI AND COTTIS EXPERIMENT	4-1
4.1.1 Setting Up the Model	4-1
4.1.2 Modelled Results	4-4
4.2 VALDES (1987) EXPERIMENTS - ACETATE SYSTEM	4-6
4.2.1 Setting Up the Model	4-6
4.2.2 Customization of the Code for Valdes Acetate Problem	4-9
4.2.3 Modelled Results	4-10
4.3 VALDES EXPERIMENT - SULFURIC ACID SYSTEM	4-15
4.3.1 Customization of the Code for Valdes Sulfate Problem	4-16
4.3.2 Modelled Results	4-16
5 CONCLUSION	5-1
6 REFERENCES	6-1
APPENDIX	
A STRUCTURE OF CODE	
B SUMMARY OF <i>MARIANA</i> SUBROUTINE	
C OPERATING INSTRUCTIONS	

FIGURES

Figure		Page
2-1	Schematic of Model Geometry	2-3
3-1	Flow diagram	3-2
4-1	Experimental and predicted pH after 90 hours assuming different constant anodic current densities for Alavi and Cottis (1987) experiment	4-4
4-2	Experimental and predicted pH 7.5 mm into the crevice assuming different constant anodic current densities for Alavi and Cottis (1987) experiment	4-5
4-3	Experimental and predicted potential drop after 90 hours assuming different constant anodic current densities for Alavi and Cottis (1987) experiment	4-5
4-4	Experimental and predicted potential drop 7.5 cm into the crevice using different constant anodic current densities for the Alavi and Cottis (1987) experiments	4-6
4-5	Measured current density versus potential for iron in acetate buffer solution (Valdes, 1987)	4-9
4-6	Experimental and predicted corrosion potentials using different activity coefficient calculation methods for iron in acetate solution polarized at 0.844 V_{SHE} (Valdes, 1987, experiment)	4-10
4-7	Experimental and predicted corrosion potentials with and without complexation for iron in acetate solution polarized to 0.844 V_{SHE} (Valdes, 1987, experiment)	4-11
4-8	Anodic current density at metal/solution interface for iron acetate solution polarized to 0.844 V_{SHE}	4-12
4-9	Predicted species concentration for iron in acetate solution polarized to 0.844 V_{SHE}	4-12
4-10	Experimental and predicted potentials for iron in acetate solution polarized at 1.244 V_{SHE} using different activity coefficient calculation methods (Valdes, 1987, experiment)	4-13
4-11	Experimental and predicted corrosion potentials with and without complexation for iron in acetate solution polarized at 1.244 V_{SHE} (Valdes, 1987, experiment)	4-13
4-12	Anodic current density at metal/solution interface for the 1.244 V_{SHE}	4-14
4-13	Predicted species concentration for iron in acetate solution polarized to 1.244 V_{SHE}	4-14
4-14	Measured anodic current density versus potential for iron in sulfuric acid solution (Valdes, 1987)	4-17
4-15	Experimental and predicted corrosion potentials with and without complexation for iron in sulfuric acid solution (Valdes, 1987, experiment)	4-17
4-16	Anodic current density at metal/solution interface for iron in sulfuric acid solution (Valdes, 1987, experiment)	4-18
4-17	Predicted species concentration for iron in sulfuric acid solution (B-dot equation)	4-18

LIST OF TABLES

Table		Page
4-1	Properties of aqueous species in solution used by Alavi and Cottis (1987)	4-3
4-2	Properties of aqueous species in acetate solution used by Valdes (1987)	4-7
4-3	Diffusion coefficients adjusted for viscosity	4-8
4-4	Properties of sulfuric acid solution species	4-14

ACKNOWLEDGEMENTS

The authors would like to thank a number of contributors to this work. Budhi Sagar suggested the upwinding scheme for improved numerical stability. Gustavo Cragolino and Narasi Sridhar provided assistance and useful discussions of thermodynamic data and model formulation. Bill Murphy provided help with thermodynamic data. Dave Turner and Gustavo Cragolino were technical reviewers of the document.

This report was prepared to document work performed by the CNWRA for Nuclear Waste Regulatory Analyses (CNWRA) for the Nuclear Regulatory Commission (NRC) under Contract NRC-02-88-005. The activities reported here were performed on behalf of the NRC Office of Nuclear Materials Safety and Safeguards. The report is an independent product of the CNWRA and does not necessarily reflect the views or regulatory position of the NRC.

DISCLAIMER

This report was prepared as an account of work sponsored by an agency of the United States Government. Neither the United States Government nor any agency thereof, nor any of their employees, nor any of their contractors, subcontractors, or their employees, makes any warranty, expressed or implied, or assumes any legal liability or responsibility for the accuracy, or any third party's use or the results of such use of any information, apparatus, product, or process disclosed, or represents that its use would not infringe privately owned rights. Reference herein to any specific commercial product, process, or service by trade name, trademark, manufacturer, or otherwise, does not necessarily constitute or imply its endorsement, recommendation, or favoring by the United States Government or any agency thereof or its contractors or subcontractors. The views and opinions of authors expressed herein do not necessarily state or reflect those of the United States Government or any agency thereof.

1 INTRODUCTION

In accordance with the provisions of the Nuclear Waste Policy Act (NWPA), as amended, the Nuclear Regulatory Commission (NRC) has the responsibility of granting a license for the first (and subsequent, if any) geologic repository for high-level nuclear waste (HLW). The Center for Nuclear Waste Regulatory Analyses (CNWRA) at Southwest Research Institute (SwRI) is a Federally Funded Research and Development Center (FFRDC) created to support the NRC in its mission of licensing the repository. To meet its licensing function, the NRC will review the application submitted by the Department of Energy (DOE). One of the critical sections of the license application will deal with the assessment of the future performance of the repository system which has to meet the system requirements in 10 CFR 60.112 and the subsystem Particular Barriers requirements in 10 CFR 60.113.

In order to develop capabilities to review the performance assessment in DOE's license application, the staffs of the NRC and the CNWRA are engaged in developing and applying performance assessment methods and models to existing data. Later, at the time of license application review, these methods may be used to conduct an independent performance assessment, if the NRC elects to do so.

The Engineered Barriers System Element addresses the subsystem performance requirements in 10 CFR 60.113 for containment and gradual release rate. To support the evaluation of these requirements, software development activities are underway at the CNWRA. The detailed modelling in support of the containment and gradual release rate performance assessment is provided by the Engineered Barrier System Performance Assessment Codes (EBSPAC) development program. Together with the system source term code development, *SOTEC*, and the EBSPAC development, comprehensive and integrated system/subsystem performance assessments can be conducted.

Twitch is being developed as part of the modeling effort conducted under the EBSPAC program. Calculations and models related to engineered barriers behavior must often consider mass transport coupled to chemical reaction in aqueous systems. Examples are localized corrosion of metallic containers, spent fuel dissolution as affected by transport processes, degradation of concrete in the presence of ground water, and release of contaminants from engineered waste forms. In recognition of the requirement for reactive transport calculations in a variety of engineered barriers performance and research models, the Engineered Barriers Element has developed a reactive transport model, *Twitch*. *Twitch* considers diffusion, electromigration, electrochemical reactions, and reactions in solution. The code is written in finite difference format and coupled to the equilibrium solver *Mariana* (Walton and Kalandros, 1992) to maintain chemical equilibrium at each node. The code has a simple input/output structure and logic that facilitates application of the code to many different problems.

In order to keep the code general, *Twitch* has no built-in database. Instead, the required thermodynamic and transport data are read from an input deck. Reactions are input in the form of a stoichiometric matrix. Only reactions passed in the matrix are considered and all homogeneous reactions are solved to equilibrium. Heterogeneous reactions are subject to mass balance and kinetic constraints and may not reach equilibrium. For example, if all the mass of a particular solid is depleted, the reaction in which the solid dissolves is automatically removed from consideration.

The code is modular in format to facilitate customization for different tasks. At a later date, a two- or three-dimensional sister code without current in solution may be developed. The initial version of *Twitch*

was optimized for consideration of crevice corrosion problems but is applicable to a wide range of other applications.

In the corrosion area, the model breaks new ground in two areas (i) equations for moderately concentrated solutions, including individual ion activity coefficients and transport by chemical potential gradients, are used rather than equations for dilute solutions, and (ii) the model is capable of handling active, transient crevice corrosion. The other transient corrosion models only simulate only the passive metal case. These capabilities allow the model to be used for simulating crevice corrosion initiation, propagation rate, and repassivation potential.

2 THEORY

Twitch considers mass transport by diffusion and electromigration. The flux equation for diffusion and electromigration of aqueous species is (Bockris and Reddy, 1977):

$$N_i = -\frac{D_i C_i}{RT} \nabla (z_i F \phi_s + \mu_i) \quad (2-1)$$

where:

- N_i = flux of species i
- D_i = diffusion coefficient of species i
- C_i = concentration of species i
- z_i = charge of ionic species i
- μ_i = chemical potential of species i
- R = gas law constant
- T = absolute temperature
- F = Faraday constant
- ϕ_s = electrostatic potential in solution

The chemical potential is given by:

$$\mu_i = \mu_i^\circ + RT \ln \{a_i\} \quad (2-2)$$

The activity of each aqueous species is given by:

$$a_i = \gamma_i C_i \quad (2-3)$$

This can be expanded to:

$$\begin{aligned} N_i &= -\frac{z_i D_i F}{RT} C_i \nabla \phi_s - \frac{D_i C_i}{RT} \nabla (\mu_i^\circ + RT \ln \{\gamma_i C_i\}) \\ &= -\frac{z_i D_i F}{RT} C_i \nabla \phi_s - \frac{D_i C_i}{RT} \cdot \frac{RT \cdot (\gamma_i \nabla C_i + C_i \nabla \gamma_i)}{\gamma_i C_i} \\ &= -\frac{z_i D_i F}{RT} C_i \nabla \phi_s - \frac{D_i}{\gamma_i} (\gamma_i \nabla C_i + C_i \nabla \gamma_i) \end{aligned} \quad (2-4)$$

where μ_i° is the standard state chemical potential of species i and γ_i is the activity coefficient of species i .

The flux of ions results in a current in the solution:

$$\begin{aligned}
i_s &= F \sum_i z_i N_i = F \sum_i z_i \left[-\frac{z_i D_i F}{RT} C_i \nabla \phi_s - \frac{D_i}{\gamma_i} (\gamma_i \nabla C_i + C_i \nabla \gamma_i) \right] \\
&= -F^2 \sum_i \left[\frac{z_i^2 D_i}{RT} C_i \nabla \phi_s \right] - \sum_i \left[\frac{z_i F D_i}{\gamma_i} (\gamma_i \nabla C_i + C_i \nabla \gamma_i) \right]
\end{aligned} \tag{2-5}$$

where i_s represents the current density in solution. Solving for the potential in solution yields:

$$\nabla \phi_s = \frac{-\left(i_s + \sum_i \frac{z_i F D_i}{\gamma_i} (\gamma_i \nabla C_i + C_i \nabla \gamma_i) \right)}{\kappa} \tag{2-6}$$

$$\kappa = F^2 \sum_i \frac{z_i^2 D_i}{RT} C_i \tag{2-7}$$

In order to specify the current in solution for a particular problem, one must consider conservation of charge, and either electroneutrality or Poisson's equation for the potential. In the case of electroneutrality, there can be no storage of charge or capacitance in the solution; the solution is always electrically neutral at every point:

$$\sum_i z_i C_i = 0 \tag{2-8}$$

For one-dimensional geometry with a no-flux boundary at one end of the model domain (Figure 2-1), the current at any point by electroneutrality is:

$$i_s = \frac{\int_0^L i_e dx}{g} \tag{2-9}$$

where i_e is the current density at the metal/solution interface resulting from electrochemical reactions, g is the crevice gap or width of the simulation domain, x is the position in the domain, and L is the length of the domain. Both i_e and i_s are functions of x . Substituting Eq. (2-9) into Eq. (2-6) will maintain electroneutrality in the system. In essence, electroneutrality is used to eliminate the potential from the transport equations. Eq. (2-6) can then be used in conjunction with Eq. (2-4) to calculate the flux of each species.

For active crevice corrosion, the current density at the metal/solution interface, i_e , is generally a function of the potential, temperature, and concentrations of the aqueous species present:

$$i_e = f(E, T, C_1, C_2, \dots, C_n) \tag{2-10}$$

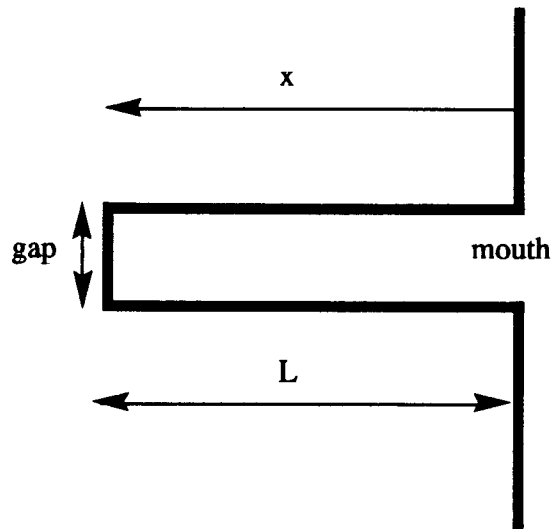


Figure 2-1. Schematic

The electrode potential or potential, E , is defined as the potential of the metal relative to the potential in solution:

$$E = \phi_m - \phi_s \quad (2-11)$$

where ϕ_m is the potential of the metal. A constant anodic current density, relatively independent of potential over a wide potential range, can be assumed for the special case of passivated metal. For either case, the principal electrochemical reaction of concern is the dissolution of metal:



where "Me" refers to a metal with n valence electrons and "e" refers to an electron. Possible cathodic reaction is the reduction of hydrogen ions:



In addition to driving the current in solution, these reactions define the flux of ions at the metal/solution interface:

$$\bar{N}_i = \frac{\alpha_i i_e}{z_i F} \quad (2-14)$$

$$\sum_i \alpha_i = 1$$

where \bar{N}_i is the flux of species i into solution at the metal/solution interface and α_i is a weighting factor indicating the relative rate of production of species i . The α_i is based upon metal composition making the assumption of congruent dissolution.

Assuming the flux at the metal/solution interface is averaged over the crevice gap (thereby becoming a volumetric source term), the material balance at any point is given by:

$$\frac{\partial C_i}{\partial t} = -\nabla \cdot N_i + \frac{\bar{N}_i}{g} + R_i \quad (2-15)$$

where R_i represents the rate at which species i is produced through chemical reactions per unit volume in solution. Since the concentration and potential gradient depend upon each other the governing equations are inherently nonlinear, even without consideration of chemical reactions.

3 IMPLEMENTATION OF THEORY

Twitch operates on the assumption that the characteristic times of homogeneous chemical reactions in aqueous solutions are much shorter than those of mass transport or corrosion processes. Thus, the aqueous solution is usually assumed to be at equilibrium. For many systems, this is either a valid assumption or a useful approximation. Given the local equilibrium assumption, the equations governing mass transport and corrosion may be decoupled from those governing equilibrium reactions. This decoupling substantially simplifies numerical solution of the equations. The local equilibrium assumption is the default in *Twitch* but is not required for all reactions. A wide variety of kinetic formulations can be accommodated through customization of the *corrode* subroutine.

The decoupled solution methodology can become unstable at large time steps. Additionally, even when the equations are stable, large time steps can lead to inaccurate solutions. The stability of the method is dependent upon how the reaction equations are written. In general, equations should be written in terms of the species present in the greatest amount. For example, in acidic systems, hydrolysis reactions work better when written in terms of the hydrogen ion. In alkaline systems, the reactions are preferably written in terms of the hydroxide ion.

The default version of *Twitch* is optimized for the one-dimensional crevice corrosion problem with depth of the crevice being the dimension. The crevice gap is specified as an input, and concentrations are averaged or lumped in this second dimension. A spatial finite difference scheme is used to convert the governing partial differential equations into ordinary differential equations (ODE) at each node. The present version of the code then integrates in time using one of the three specified ODE solvers with monitored accuracy and step size control. If the desired accuracy is not achieved, then the step size is reduced automatically. This step size control only pertains to the transport equations; thus, the time step specified in the input deck actually determines the time steps for decoupling the equations into chemical reaction and transport steps.

Boundary conditions are currently specified as no flux at the high end of the domain ($x = L$) and fixed concentration at the lower end of the domain ($x = 0$). These boundary conditions are consistent with and required by Eq. (2-9) in order to estimate the current anywhere within the domain. If no current is present, any boundary conditions could be applied; however, other boundary conditions are not presently implemented in the code.

The solution sequence for each time step is summarized as follows (Figure 3-1):

- Calculate the current in solution (i_s) at each nodal interface [Eq. (2-9)]
- Estimate the potential gradient and potential in solution ($\nabla\phi_s$) at each node [Eq. (2-6)]
- Iterate by relaxation on the above two steps until the potential converges within tolerance
- Calculate the flux of each ionic species through the metal/solution interface (\bar{N}_i) at each node [Eq. (2-14)]
- Calculate the flux of each aqueous species (N_i) at each nodal interface [Eq.(2-4)]
- Simultaneously solve the mass transport equations for the concentration of each aqueous species (C_i) at each node [mass transport part of Eq. (2-15)]
- Equilibrate the solution at each node through a call to *Mariana* (Walton and Kalandros, 1992) [chemical reaction part of Eq. (2-15)]
- Apply assumption of electroneutrality to correct for numerical errors [Eq. (2-8)]

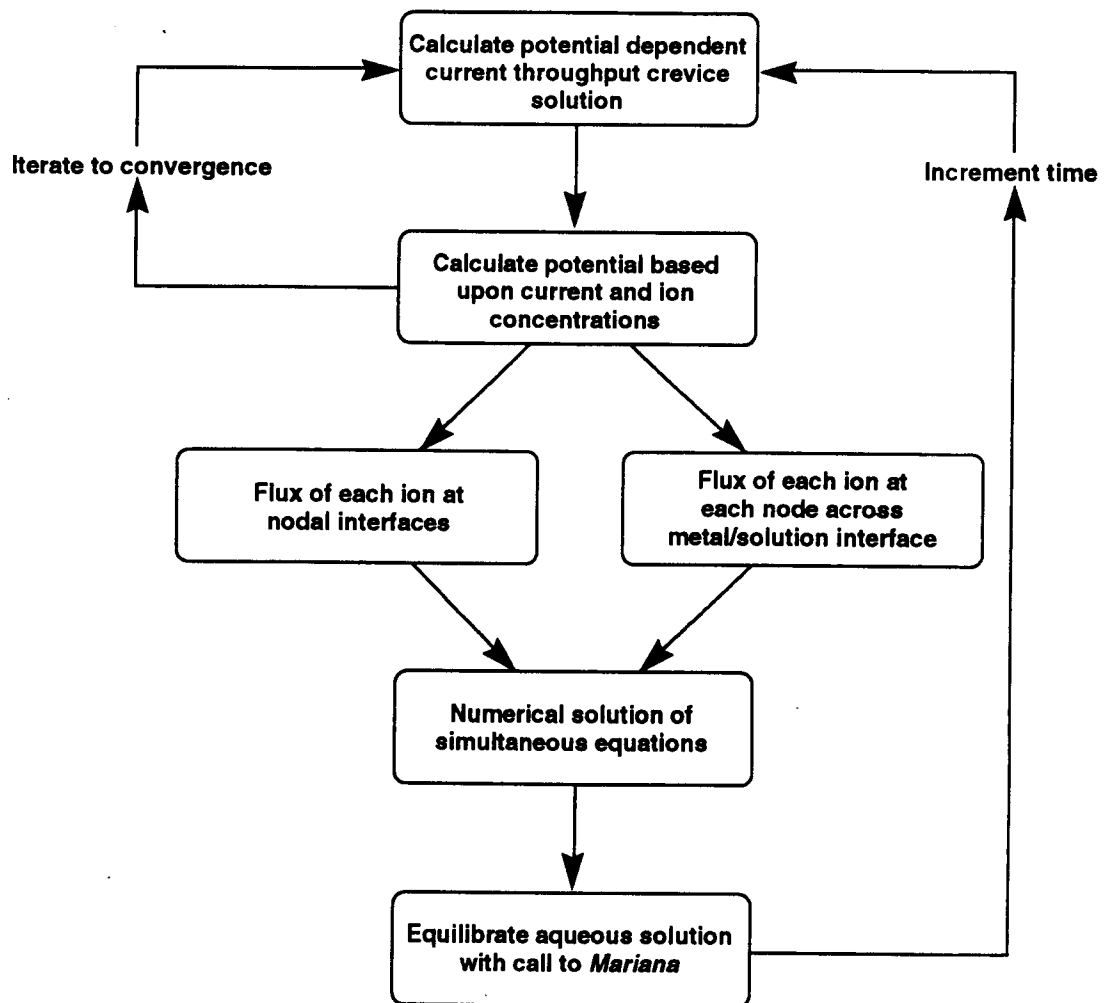


Figure 3-1. Flow diagram of solution sequence

Twitch calls various subroutines to accomplish these tasks. These subroutines are described in the following sections.

3.1 CORROSION AND CALCULATION OF CURRENT IN SOLUTION

The *corrode* subroutine is responsible for the corrosion reactions at the metal/solution interface. The subroutine is isolated from the rest of the code because customization of the routine may be required for some problems. The requirement for customization results from the highly variable nature of the

expressions for electrochemical reactions at the metal/solution interface. *Twitch* assumes that the *corrode* subroutine will estimate the flux of each ionic species through the metal/solution interface at each node using Eq. (2-14). Additionally, the current in solution at each nodal interface is estimated in *corrode* using Eq. (2-9). This format is consistent with any kinetic formulation including consideration of both cathodic and anodic reactions as well as active corrosion.

The default version of *corrode* assumes a constant anodic reaction rate consistent with a passivated crevice. No customization is required for this case. *Twitch* can be adapted to model non-corrosive systems by entering a zero passive current density.

3.2 POTENTIAL GRADIENT ESTIMATION

The potential gradient at each interface is estimated in the *gradient* subroutine. The interfacial concentration for calculating the potential gradient used in Eq. (2-6) is the arithmetic average of the concentration at adjacent nodes. The concentration gradient is obtained by differencing the two adjacent nodes.

The new potential at each time step is determined by averaging the previous value with the predicted value based upon the input relaxation factor. The estimates of potential in solution and potential gradient are iterated until convergence is obtained.

3.3 CALCULATION OF FLUX AND MASS TRANSPORT

The flux of aqueous species across each nodal interface is calculated using Eq. (2-4) by replacing all the concentration and γ derivatives by finite difference approximations. The mass transport part of Eq. (2-15) is thereby converted to a series of ordinary differential equations:

$$\frac{dC_i}{dt} = \frac{A}{V} (N_i^{\text{in}} - N_i^{\text{out}}) + \frac{\bar{N}_i}{g} \quad (3-1)$$

where V is volume and A is area. The flux of each ion at the metal/solution interface \bar{N}_i is estimated in the *corrode* subroutine based upon the potential and aqueous concentration at the node. The interface between nodes is defined to be at the midpoint between adjacent nodes, allowing for variable node spacing. Node spacing is specified by the user in the input deck. The interfacial concentration of each species is usually estimated by averaging concentrations at adjacent nodes. However, when high potential gradients are present, the central differencing scheme can become unstable. An effective Peclet number for the system can be defined as:

$$Pe = \frac{\left(\frac{z_i F D_i \nabla \phi_s}{RT} \right)}{\left(\frac{D_i}{\Delta x} \right)} = \frac{\Delta x z_i F \nabla \phi_s}{RT} \quad (3-2)$$

If the absolute value of the Peclet number is greater than two, an upwinding scheme is used. In the case where $z_i \nabla \phi > 0$, the interfacial concentration is assumed to be equal to the concentration at

the next higher node. When $z_i \nabla \phi < 0$ the concentration at the lower node is used. The assumption involved with upwinding is that, when electromigration is strong, relative to diffusion, the best estimate of concentration at the nodal interface is the concentration at the up gradient node.

The upwinding scheme is only first order accurate, whereas the central difference method is second order accurate. Thus some accuracy is sacrificed to obtain increased stability. Refinement of the grid can be used to eliminate the upwinding and gain increased accuracy. As with any numerical code, adequacy of the discretization can be checked by continual refinement of the grid until the answers no longer change significantly. Smaller nodal spacings are recommended at locations where concentration and potential gradients are greatest. In the case of crevice corrosion problems this will usually be near the mouth of the crevice.

The system of ordinary differential equations (ODE) can be solved with any ODE solver. Three solvers are initially included in *Twitch*, an Adams method (Hindmarsh, 1983); the Bulirsch-Stoer method (Press, *et al.*, 1986); and the 5th-order Runge-Kutta method (Press, *et al.*, 1986). The ODE solvers have the advantage of "plug-and-play" availability with automatic step size control and the ability to handle highly nonlinear equations as required for corrosion problems. This facilitates obtaining an operable code within a limited time frame. The question of which solver will work better for a particular situation has not been resolved. In future revisions other, potentially faster, numerical solution methodologies will be investigated.

3.4 EQUILIBRATION

At the end of each time step, the equilibrium assumption is applied by calling the *Mariana* subroutine (Walton and Kalandros, 1992). This call accounts for the R_i term in Eq. (2-15). *Mariana* also calculates the activity coefficient of each species. The activity coefficient can be calculated by the Davies equation (Stumm and Morgan, 1981), the B-dot Debye-Hückel equation (Helgeson, 1969), or assumed equal to unity. For unit activity coefficients, the governing equations are those corresponding to dilute solution theory.

The B-dot equation is given by:

$$\log(\gamma_i) = -Az_i^2 \frac{\sqrt{I}}{1 + a_i^o B \sqrt{I}} + \dot{B}I$$

where

- A = Debye-Hückel parameter
- I = ionic strength
- B = Debye-Hückel parameter
- a_i^o = ion size parameter for species i
- \dot{B} = B-dot parameter

The A , B , and \dot{B} parameters are calculated in *Mariana* as a function of temperature based upon data on the EQ3/6 database version (data0.com.R12) (Wolery, 1983, Wolery, *et al.*, 1990).

3.5 ERROR CORRECTION THROUGH ELECTRONEUTRALITY

The above formulation maintains electroneutrality by balancing charge at every step. However, this maintenance of electroneutrality is subject to drift related to roundoff error and numerical approximations. This is especially true when the less accurate unwinding scheme is applied. In order to prevent drift, the numerical error resulting from each time step is equally distributed among the ions in solution according to the charge density of each ion. This compensation for numerical error is *not* the primary means by which the code maintains electroneutrality; it is only a compensation for numerical errors which are otherwise compounded. The corrections applied at each time step are typically very small relative to total charge density in the solution.

4 CODE VERIFICATION AND MODEL VALIDATION

The initial version of the code has undergone limited testing. The interface to *Mariana* has been checked by verifying that the code maintains solutions at equilibrium. The finite difference solution has been checked to verify that grid refinements and smaller time steps lead to consistent solutions.

In the following sections, *Twitch* is used to model the results of several experiments described in the corrosion literature. This represents an initial effort towards model validation.

4.1 ALAVI AND COTTIS (1987) EXPERIMENT

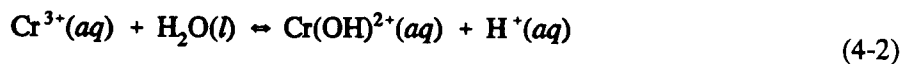
4.1.1 Setting Up the Model

Alavi and Cottis (1987) conducted an experiment concerning crevice corrosion in stainless steel (SS). The electrolyte was a 0.6 M NaCl solution at 25°C with a pH of 6.0. A plate of type 304 SS and a perspex electrode holder formed an experimental crevice measuring 8 cm deep, 2.5 cm wide and 90 μm gap. The steel was coupled to a larger piece of the same steel which was exposed to free-corrosion conditions in the aerated bulk electrolyte. The experiment lasted 164 hours.

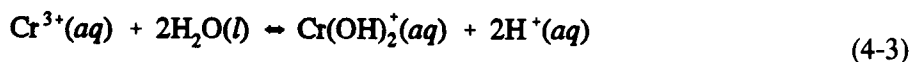
The thirteen reactions assumed to occur in the system are listed below with their equilibrium constants at 25°C:



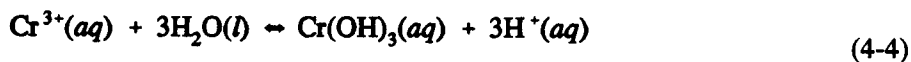
$$K = 1.01 \times 10^{-14}$$



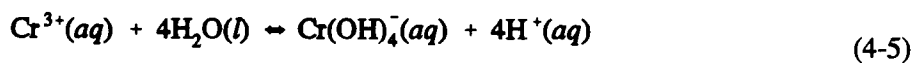
$$K = 9.97 \times 10^{-5}$$



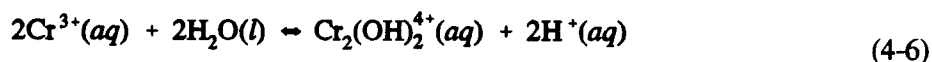
$$K = 1.99 \times 10^{-10}$$



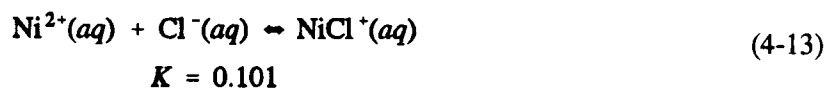
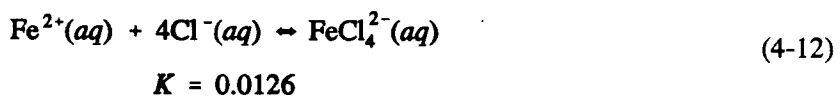
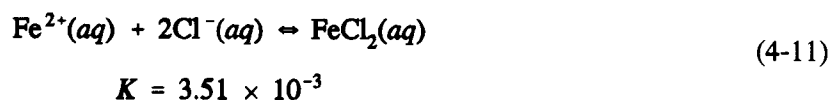
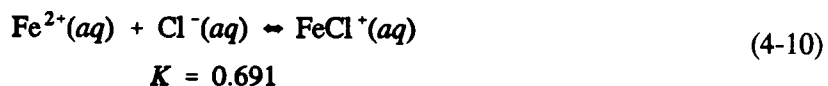
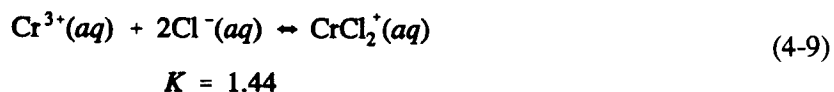
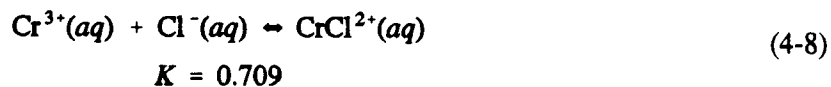
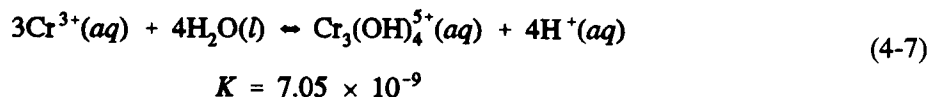
$$K = 9.95 \times 10^{-19}$$



$$K = 3.95 \times 10^{-28}$$



$$K = 8.69 \times 10^{-6}$$



These reactions involve eighteen aqueous species in addition to water. The Na^+ ion from the sodium chloride solution must also be included in the input deck for the sake of preserving electroneutrality. The properties of these twenty species are listed in Table 4-1. Thermodynamic data were taken from the EQ3/6 (Wolery, 1983, Wolery *et al.*, 1990) database version data0.com.R12. Diffusion coefficients are estimated.

The reactions assumed to occur at the metal/solution interface are:



Table 4-1. Properties of aqueous species in solution used by Alavi and Cottis (1987).

Species	ΔG_f° in (J/mol)	D (dm ² /s)	a_i° (Å)
H ₂ O(l)	-237,200	—	—
H ⁺ (aq)	0	9.3×10^{-7}	9.0
OH ⁻ (aq)	-157,300	5.0×10^{-7}	3.0
Na ⁺ (aq)	-261,900	1.3×10^{-7}	4.0
Cl ⁻ (aq)	-131,300	2.0×10^{-7}	3.0
Cr ³⁺ (aq)	-195,100	0.6×10^{-7}	5.0
Cr(OH) ²⁺ (aq)	-409,400	0.7×10^{-7}	4.5
Cr(OH) ₂ ⁺ (aq)	-614,100	0.8×10^{-7}	4.0
Cr(OH) ₃ (aq)	-803,900	0.8×10^{-7}	—
Cr(OH) ₄ ⁻ (aq)	-987,400	0.8×10^{-7}	4.0
Cr ₂ (OH) ₂ ⁴⁺ (aq)	-789,600	0.5×10^{-7}	5.5
Cr ₃ (OH) ₄ ⁵⁺ (aq)	-1,487,400	0.4×10^{-7}	6.0
CrCl ²⁺ (aq)	-325,500	0.8×10^{-7}	4.5
CrCl ₂ ⁺ (aq)	-458,600	0.8×10^{-7}	4.0
Fe ²⁺ (aq)	-91,500	0.7×10^{-7}	6.0
FeCl ⁺ (aq)	-221,900	0.8×10^{-7}	4.0
FeCl ₂ (aq)	-340,100	0.8×10^{-7}	—
FeCl ₄ ²⁻ (aq)	-605,800	0.5×10^{-7}	4.0
Ni ²⁺ (aq)	-45,600	0.7×10^{-7}	4.5
NiCl ⁺ (aq)	-171,200	0.8×10^{-7}	4.0
ΔG_f° = Gibbs Free Energy of formation D = diffusion coefficient (estimated) z = charge a_i° (Å) = ion size parameter			

These reactions are assumed to occur at relative rates proportional to the constitution of the steel; thus, the anodic current was assumed to consist of 74% Fe^{2+} , 18% Cr^{3+} , and 8% Ni^{2+} .

The simulation was run for 90 hours using the Adams solver with an input tolerance of 10^{-4} . The B-dot equation was used to determine activity coefficients. Three simulations were conducted assuming passive corrosion with three different constant anodic currents: 10^{-3} A/dm^2 , 10^{-4} A/dm^2 , and 10^{-5} A/dm^2 . The anodic current density was not measured in the experiments, thus modeling of the system requires an assumption concerning the anodic current density. The simplest assumption is a constant current density as might be expected under steady state conditions on a passivated metal. Sharland (1992) modeled the Alavi and Cottis data with the same assumption for current density. This assumption represents the evolution of pH and potential inside the crevice prior to its activation leading to accelerated crevice corrosion. Results were obtained at times of 2, 18, 24, 43, and 90 hours, corresponding to the measurements in the Alavi and Cottis experiment.

4.1.2 Modelled Results

The results for pH of the solution versus position in the crevice at 90 hours are shown in Figure 4-1. In the experimental data, the pH versus depth curve passes through a minimum and then increases at the base of the crevice. Alavi and Cottis suggested that the minimum in pH may correspond to a peak in anodic current density. Since current density is assumed to be constant, the pH minimum is not reproduced by the model. It would be possible to make the anodic current density a function of distance inside the crevice and obtain better agreement with data (i.e., use anodic current density as a fit parameter). However, little would be accomplished thereby. This figure can be compared directly with Figure 3 in Sharland (1992) based upon *CHEQMATE* code simulations. Similar results are obtained from both models.

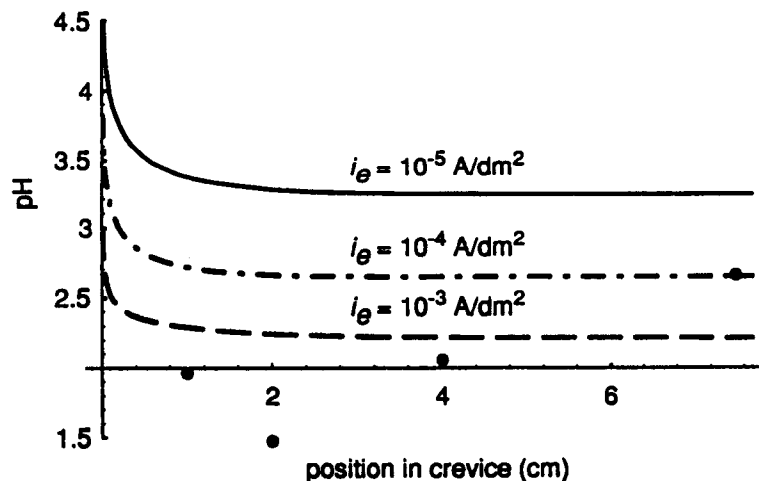


Figure 4-1. Experimental (•) and predicted pH after 90 hours assuming different constant anodic current densities for Alavi and Cottis (1987) experiment

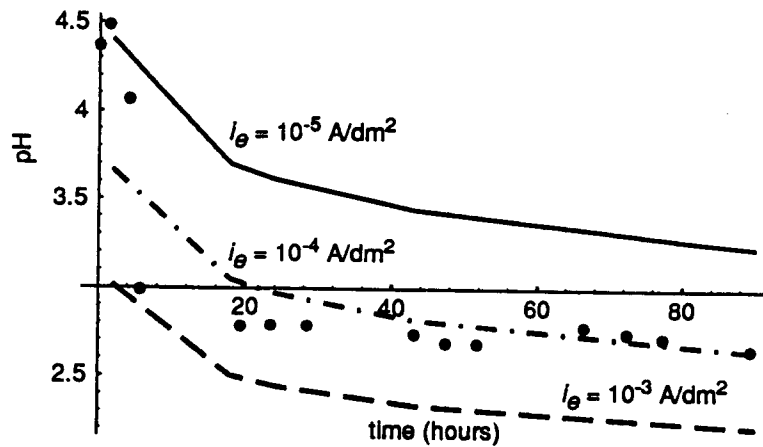


Figure 4-2. Experimental (●) and predicted pH 7.5 mm into the crevice assuming different constant anodic current densities for Alavi and Cottis (1987) experiment

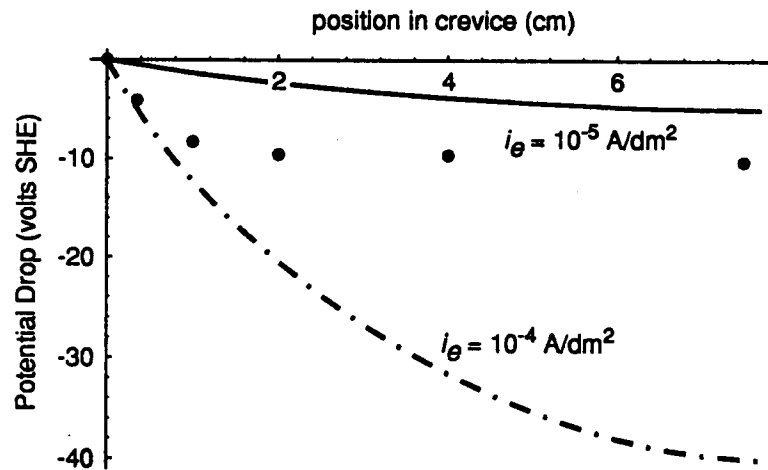


Figure 4-3. Experimental and predicted potential drop after 90 hours assuming different constant anodic current densities for Alavi and Cottis (1987) experiment

Figure 4-2 shows pH of the solution in a position 7.5 cm into the crevice versus time. Most of the experimental pH values lie near the predicted values at a current density of 10^{-4} A/dm².

Figure 4-3 shows the potential drop in the solution versus position in the crevice after 90 hours. The potential drop agrees reasonably well with model predictions assuming a current density between 10^{-4} and 10^{-5} A/dm². Figure 4-4 shows the results for potential drop in the solution 7.5 cm into the crevice versus time. The model predicts that, at constant anodic current density, the potential drop will decrease with time as the crevice solution becomes more concentrated. The experimental values lie intermediate between the 10^{-4} and 10^{-5} A/dm² predicted values.

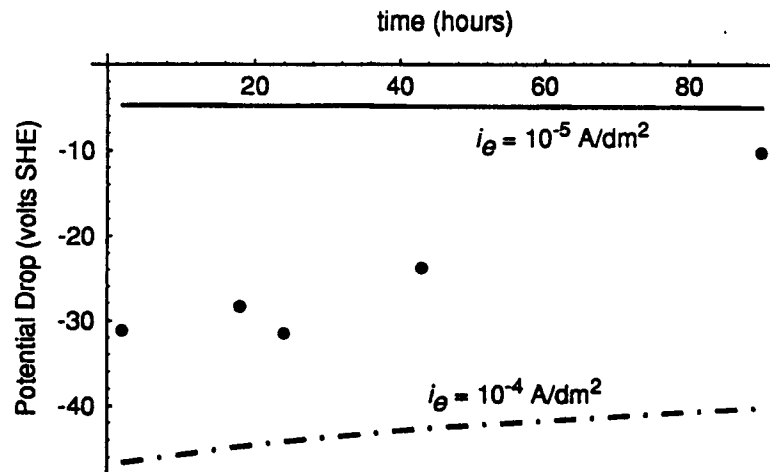


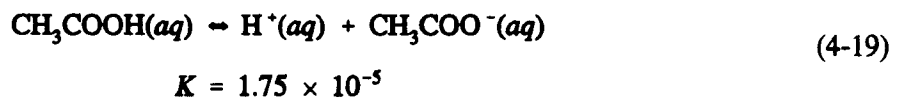
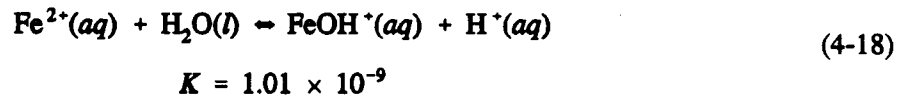
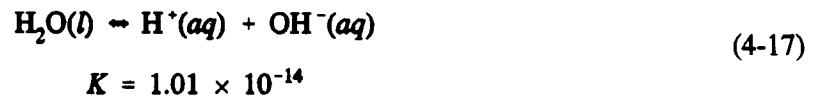
Figure 4-4. Experimental and predicted potential drop 7.5 cm into the crevice using different constant anodic current densities for the Alavi and Cottis (1987) experiments

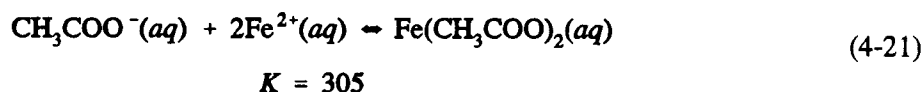
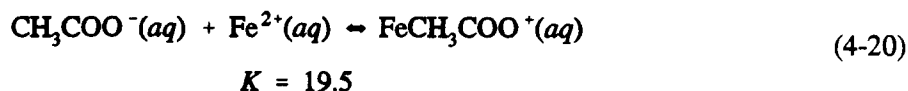
4.2 VALDES (1987) EXPERIMENTS - ACETATE SYSTEM

Valdes (Valdes, 1987; Valdes and Pickering, 1987) conducted several experiments involving crevice corrosion of iron in electrolyte solutions. The experimental crevice was 10 mm deep, 5 mm wide and with a gap of 0.5 mm, with iron metal on one side. A perpendicular section of the iron measuring 5 mm by 20 mm at the surface of the crevice was anodically polarized to different values. The experiments were carried out using first an acetate buffer solution and then a sulfuric acid solution.

4.2.1 Setting Up the Model

The acetate buffer solution consisted of equal parts 0.5 M acetic acid and 0.5 M sodium acetate solution at 25°C. This formed a buffer solution with pH 4.8. The five principal reactions occurring in the system are listed below with their equilibrium constants at 25°C:





These reactions involve seven aqueous species as well as water and one solid. In addition, the Na^+ ion from the sodium acetate solution must also be included in the input deck for the sake of preserving electroneutrality. The properties of these ten species are listed in Table 4-2. Thermodynamic data was obtained from the Eq. (2-5) database (Version: data0.com.R12), Wolery, 1983.

Table 4-2. Properties of aqueous species in acetate solution used by Valdes (1987).

Species	ΔG_f° in (J/mol)	D_o (dm ² /s)	a_i° (Å)
$\text{H}_2\text{O}(l)$	-237,200	—	—
$\text{H}^+(aq)$	0.0	9.3×10^{-7}	9.0
$\text{OH}^-(aq)$	-157,300	5.3×10^{-7}	3.0
$\text{Fe}^{2+}(aq)$	-91,500	0.7×10^{-7}	6.0
$\text{FeOH}^+(aq)$	-277,400	1.0×10^{-7}	4.0
$\text{CH}_3\text{COOH}(aq)$	-396,500	1.1×10^{-7}	—
$\text{CH}_3\text{COO}^-(aq)$	-369,300	1.1×10^{-7}	4.0
$\text{CH}_3\text{COOFe}^+(aq)$	-468,200	1.1×10^{-7}	4.0
$\text{Fe}(\text{CH}_3\text{COO})_2(aq)$	-844,300	1.1×10^{-7}	4.0
$\text{Na}^+(aq)$	-261,900	1.3×10^{-7}	4.0
ΔG_f° = Gibbs Free Energy of formation D_o = diffusion coefficient (estimated) z = charge a_i° (Å) = ion size			

Since water is present everywhere in excess, it will not diffuse significantly; thus, it was removed from consideration in the mass transport step.

Vitagliano and Lyons (1956) indicate a viscosity 1.112 times that of pure water for one molar acetate solutions. The diffusivity of an aqueous species is inversely related to the solution viscosity, according to the Stokes-Einstein equation:

$$D = D_o \frac{\eta_o}{\eta} \quad (4-22)$$

where:

D	=	diffusion coefficient in solution
D_o	=	diffusion coefficient in pure water
η	=	viscosity in solution
η_o	=	viscosity in pure water

Table 4-3 gives the diffusion coefficients of the various species taking into account the higher viscosity of the acetate solution.

Table 4-3. Diffusion coefficients adjusted for viscosity

Species	D (dm ² /s)
H ₂ O(l)	—
H ⁺ (aq)	8.36×10^{-7}
OH ⁻ (aq)	4.77×10^{-7}
Fe ²⁺ (aq)	0.63×10^{-7}
FeOH ⁺ (aq)	0.90×10^{-7}
CH ₃ COOH(aq)	1.08×10^{-7}
CH ₃ COO ⁻ (aq)	1.08×10^{-7}
CH ₃ COOFe ⁺ (aq)	1.08×10^{-7}
Fe(CH ₃ COO) ₂ (aq)	1.08×10^{-7}
Na ⁺ (aq)	1.17×10^{-7}

The only reaction assumed to occur at the metal/solution interface is:



Thus, ferrous iron (Fe²⁺) is the sole constituent of the anodic current.

As mentioned before, the solution was equal parts 0.5 M CH₃COOH and 0.5 M NaCH₃COO. Thus, the boundary conditions at the mouth of the crevice are approximately 0.5 molal Na⁺, 0.5 molal CH₃COO⁻, and 0.5 molal CH₃COOH.

The simulation was run for 30 minutes using the Bulirsch-Stoer solver with an input tolerance of 10⁻⁴. Two runs were made using different methods for determining the activity coefficients: one assuming the ideal case (activity coefficients all set to 1) and one using the B-dot equation (Walton and

Kalandros, 1992). A third run was made using the B-dot equation and omitting Eqs. (4-18), (4-20), and (4-21) and from the input deck; that is, no complexation of Fe^{2+} ions was assumed to occur.

Valdes conducted the experiment with the system anodically polarized to several different values. The *Twitch* simulation was run for potentials of 0.844 volts (SHE) and 1.24+ volts (SHE). Since *Twitch* is only valid for inside the crevice, experimental values for the potential at the mouth of the crevice were used as the fixed boundary conditions; these values were 0.68 volts (SHE) and 0.92 volts (SHE), respectively. A relaxation factor of 0.2 was used for the prediction of the potential in solution.

4.2.2 Customization of the Code for Valdes Acetate Problem

The default version of the code assumes a constant anodic current density; this models the case of passive conditions established before the initiation of crevice corrosion. In the Valdes experiments, active crevice corrosion was observed. Valdes measured the anodic current density as a function of potential for both solutions he studied; the results for the acetate solution are shown in Figure 4-5. To customize the code to model the active corrosion, this curve was discretized and added to the *corrode* subroutine. This version of the subroutine first predicts the value of the potential in solution and then uses it to determine the current density at the metal solution interface. Values for the current density are obtained by linear interpolation between the base-10 logarithm of current density versus potential. The current density is assumed to remain constant for values of potential beyond the domain of the experimental data. Since *Twitch* is written in terms of the potential in solution, the potential of the metal must be defined to specify the corrosion potential. Since the conductivity of metal is large relative to that of the solution, the potential may be assumed to be constant everywhere within the metal. A value of zero was arbitrarily assigned to the potential of the metal; thus, the potential in solution is the negative of the corrosion potential.

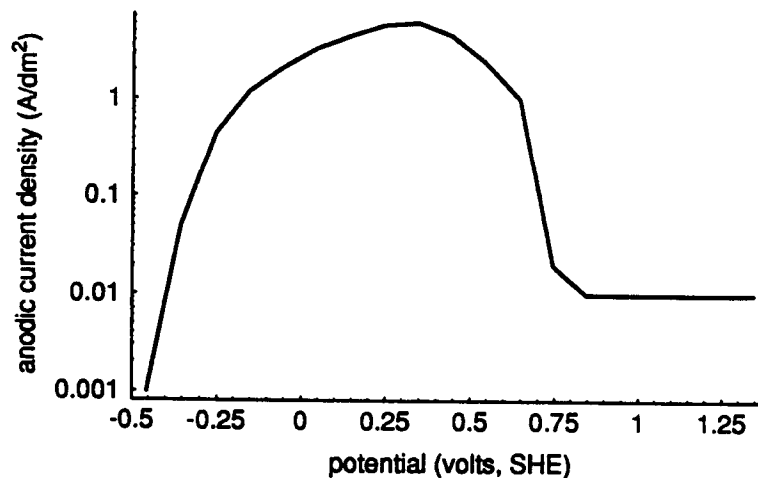


Figure 4-5. Measured current density versus potential for iron in acetate buffer solution (Valdes, 1987)

4.2.3 Modelled Results

Unlike the simulations of the Alavi and Cottis data where the current density was unknown, the Valdes data set is complete. All parameters in the Valdes simulations represent data obtained outside the crevice (i.e., without introducing fudge or fit parameters). Thus the Valdes simulations can be viewed as model predictions. Figure 4-6 shows a comparison of experimental and predicted results for the B-dot and dilute solution activity coefficient methods using the 0.68-V boundary potential (external polarization of the system to 0.844 V). Both simulations lie within the scatter of the experimental data. Interestingly, the movement from dilute solution theory to a more rigorous treatment with activity coefficients and mass transport by chemical potential gradients has relatively little influence on the model predictions.

Twitch is only valid for the inside of the crevice. However, Valdes observed significant potential drops in the bulk solution outside the crevice mouth. Since concentration gradients in the bulk solution should be small, Ohm's law may be used to estimate the potential drops. Applying Ohm's Law leads to Laplace's equation for the potential:

$$\nabla^2 \phi_s = 0 \quad (4-24)$$

PORFLO, a software package designed for groundwater applications (Runchal, *et al.*, 1985), was used to solve this equation in two dimensions outside the crevice. The following boundary conditions were applied:

- constant potential at the crevice mouth equal to the experimental value,
- an applied potential at distance in the solution at distance, and
- (no flux) on the exposed metal surface.

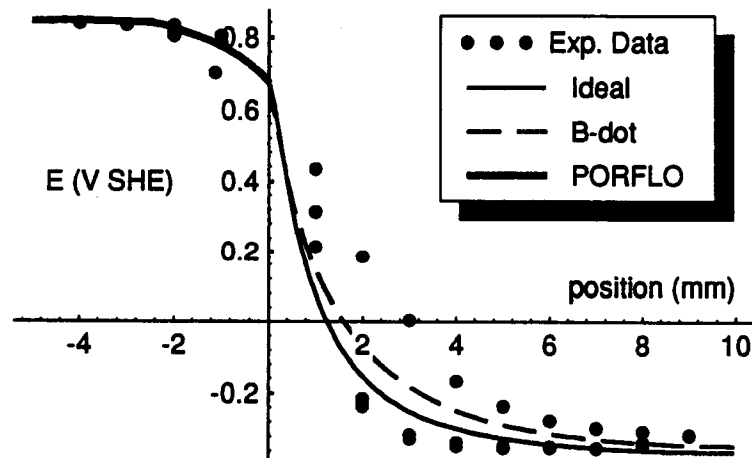


Figure 4-6. Experimental and predicted potentials using different activity coefficient calculation methods for iron in acetate solution polarized at 0.844 V_{SHE} (Valdes, 1987, experiment)

In Figure 4-6, negative values represent positions outside the crevice calculated with PORFLO.

Figure 4-7 compares the results with and without the complexation reactions [Eqs. (4-18), (4-20), and (4-21)]. The complexation reactions clearly have a large influence on the predicted potential in the solution. The complexes reduce the charge density in the solution, thereby maintaining the large potential drop even as the solution becomes more concentrated.

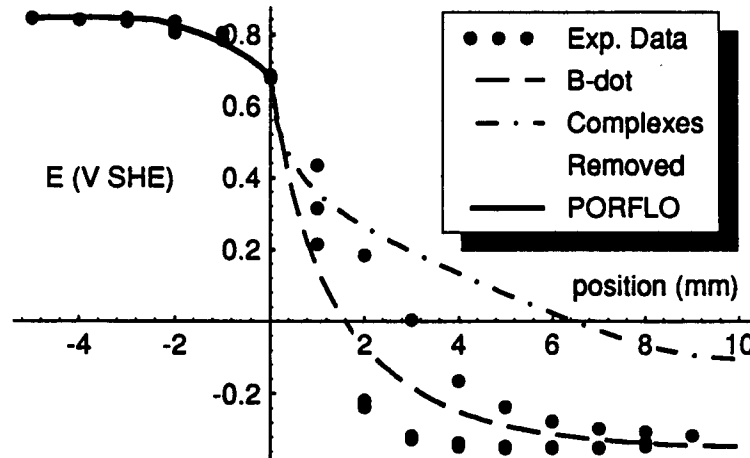


Figure 4-7. Experimental and predicted potentials with and without complexation for iron in acetate solution polarized to $0.844 V_{SHE}$ (Valdes, 1987, experiment)

Also of interest is the anodic current density. Figure 4-8 shows the simulated anodic current density after 30 minutes. The active/passive transition occurs just inside the crevice mouth. The corrosion rate peaks soon after this transition and then drops off sharply deeper into the crevice.

Figure 4-9 illustrates the concentrations of various species at the end of the 30-minute period. The ferrous ions in the solution are mostly in the form of the $Fe(CH_3COO)_2$ complex. Note that the solution is not yet at steady-state. The concentrations at the base largely reflect the initial and boundary conditions. The influence of flux at the metal/solution interface on concentrations in the system can be understood by viewing Figures 4-8 and 4-9 simultaneously.

Figures 4-10 to 4-13 represent the same calculations at a potential of $1.244 V_{SHE}$. The transition from passive to active corrosion occurs just inside the crevice. The transition occurs somewhat deeper into the crevice than before because of the higher boundary potential. The corrosion rate again peaks soon after this transition and then drops off sharply deeper into the crevice.

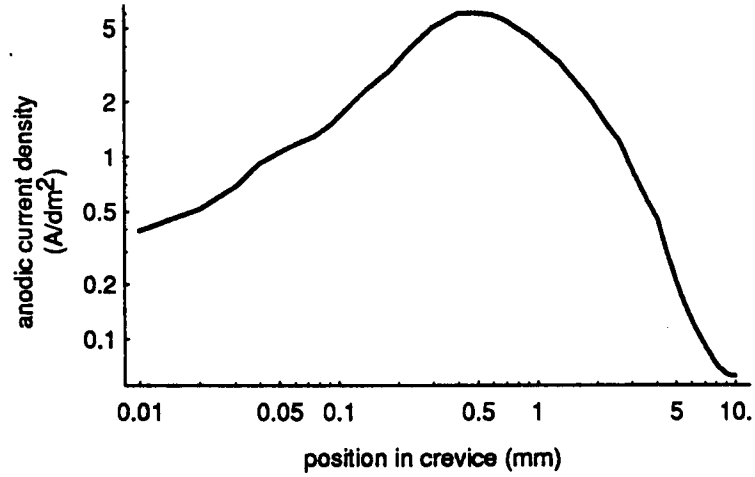


Figure 4-8. Predicted anodic current density at metal/solution interface for iron acetate solution polarized to 0.844 V_{SHE}

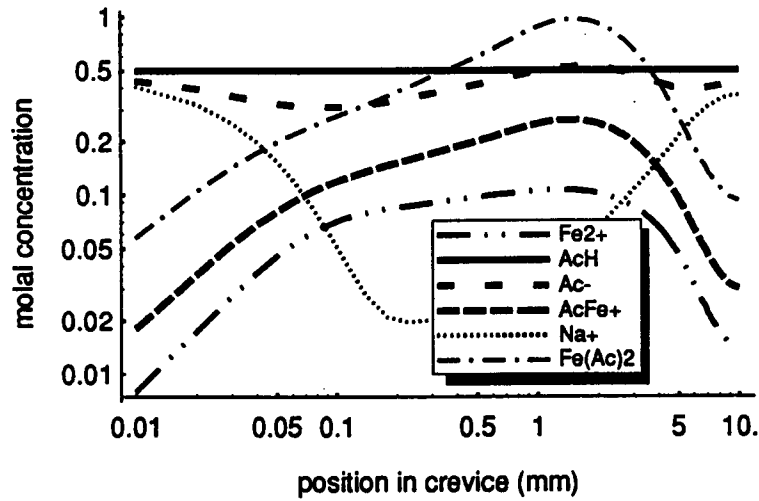


Figure 4-9. Predicted species concentration for iron in acetate solution polarized to 0.844 V_{SHE}

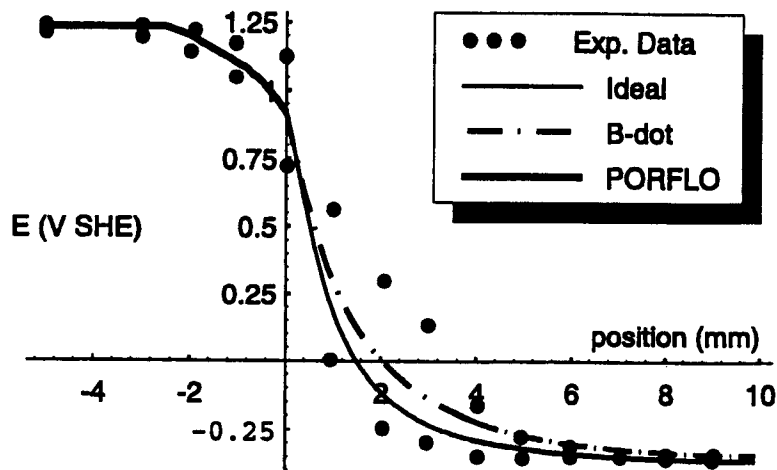


Figure 4-10. Experimental and predicted potentials for iron in acetate solution polarized at 1.244 V_{SHE} using different activity coefficient calculation methods (Valdes, 1987, experiment)

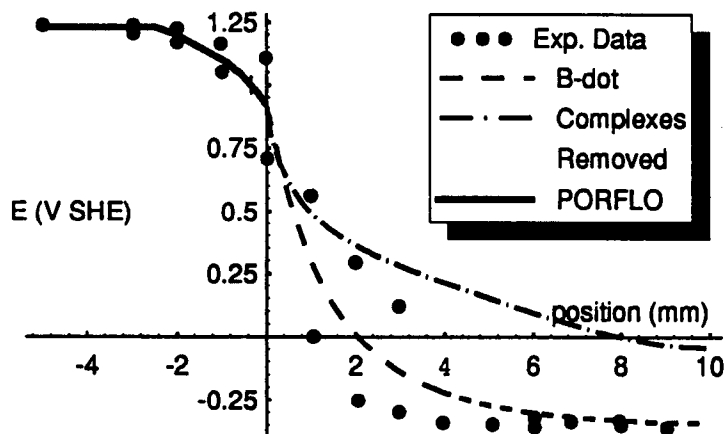


Figure 4-11. Experimental and predicted potentials with and without complexation for iron in acetate solution polarized at 1.244 V_{SHE} (Valdes, 1987, experiment)

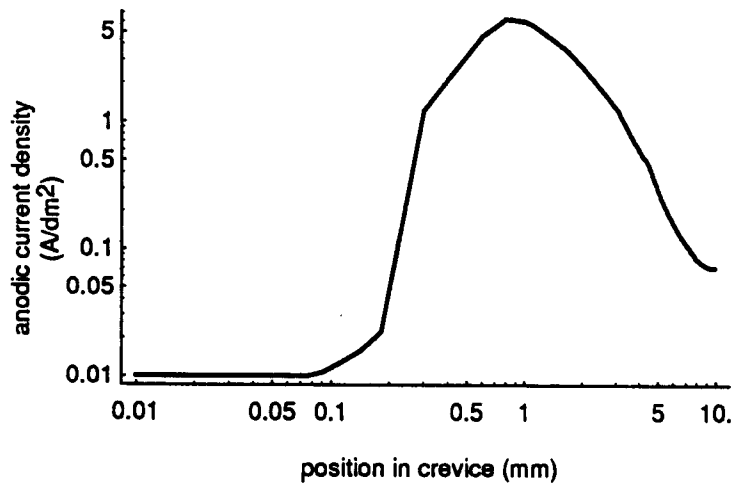


Figure 4-12. Predicted anodic current density at metal/solution interface for iron in acetate solution polarized to 1.244 V_{SHE}

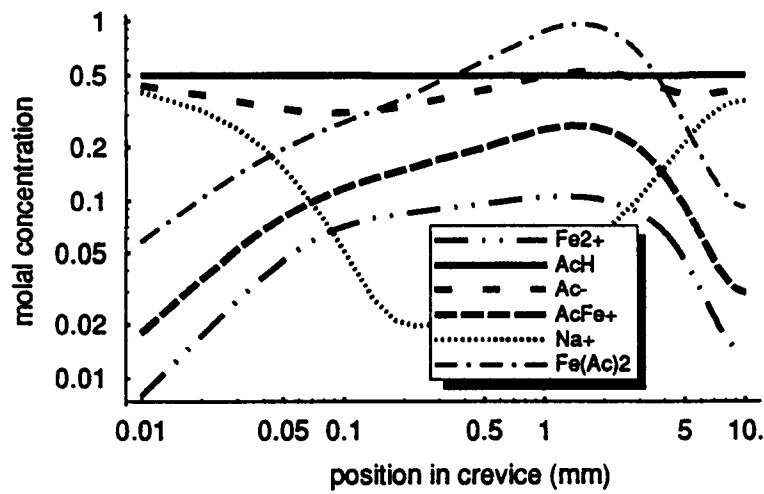
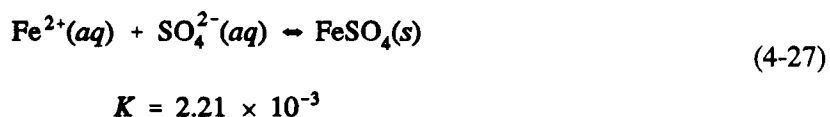
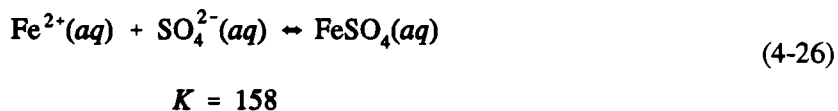
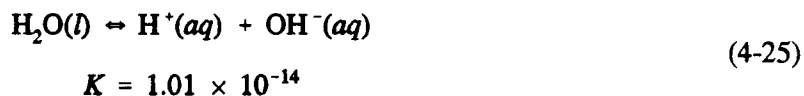


Figure 4.13. Predicted species concentration for iron in acetate solution polarized to 1.244 V_{SHE}

4.3 VALDES EXPERIMENT - SULFURIC ACID SYSTEM

Valdes also performed experiments with sulfuric acid electrolyte in the same machined crevice. The sulfuric acid solution was a 0.001 M sulfuric acid at 25°C. The three principle reactions involved are listed with their equilibrium constants 25°C:



These reactions involve five aqueous species as well as water and one solid. The properties of these species are listed in Table 4-4.

Table 4-4. Properties of sulfuric acid solution species

Species	ΔG_f° (J/mol)	D (dm ² /s)	a_i° (Å)
H ₂ O(l)	-237,200	—	—
H ⁺ (aq)	0.0	9.3×10^{-7}	9.0
OH ⁻ (aq)	-157,300	5.3×10^{-7}	3.0
Fe ²⁺ (aq)	-91,500	0.7×10^{-7}	6.0
SO ₄ ²⁻ (aq)	-744,500	1.1×10^{-7}	4.0
FeSO ₄ (aq)	-848,500	0.8×10^{-7}	—
FeSO ₄ (s)	-820,800	—	—

ΔG_f° = Gibbs Free Energy of formation
 D = diffusion coefficient (estimates)
 z = charge
 a_i° (Å) = ion size parameter

Since water is present everywhere in excess, it will not diffuse significantly; thus, it was removed from consideration in the mass transport step.

The only reaction assumed to occur at the metal/solution interface is:



Thus, ferrous iron (Fe^{2+}) is the sole constituent of the anodic current.

As mentioned before, the solution was 0.001 M sulfuric acid. Thus, the boundary conditions at the mouth of the crevice are approximately 0.002 molal H^{+} and 0.001 molal SO_4^{2-} .

The simulation was run for 30 minutes using the Bulirsch-Stoer solver with an input tolerance of 10^{-4} . Two runs were made using different methods for determining the activity coefficients: one assuming the ideal case (activity coefficients all set to 1) and one using the B-dot equation (Walton and Kalandros, 1992). A third run was made using the B-dot equation and omitting Eq. (4-26) from the input deck; that is, no complexation of Fe^{2+} ions was assumed to occur.

Valdes conducted the experiment with the system anodically polarized to several different values. The *Twitch* simulation was run for a potential of 0.844 volts (SHE). Since *Twitch* is only valid for inside the crevice, an experimental value for the potential at the mouth of the crevice was used as the fixed boundary condition; this value was -0.036 volts (SHE). A relaxation factor of 0.2 was used for the prediction of the potential in solution.

4.3.1 Customization of the Code for Valdes Sulfate Problem

The default version of the code assumes a constant anodic current density; this models the case of passive corrosion prior to crevice corrosion initiation. In the Valdes experiments, active crevice corrosion was observed. Valdes measured the anodic current density as a function of potential for both of the solutions he studied; the results for the sulfuric acid solution are shown in Figure 4-14. This curve was discretized and added to the *corrode* subroutine.

4.3.2 Modelled Results

Figure 4-15 compares the experimental results and the predicted results with and without the aqueous complexation reaction [Eq. (4-26)]. A third simulation used the ideal assumption for activity coefficients, but the results are not given here because they are indistinguishable from the B-dot results.

Figure 4-16 shows the simulated anodic current density after 30 minutes. The transition from passive to active corrosion appears to have occurred just outside of the crevice. The anodic current density drops slowly at first but then decreases abruptly.

Figure 4-17 illustrates the concentrations of various species at the end of the 30 minute period. Note that the solution is not yet at steady-state. At steady state the ion concentrations at depth would not be equal to initial values.

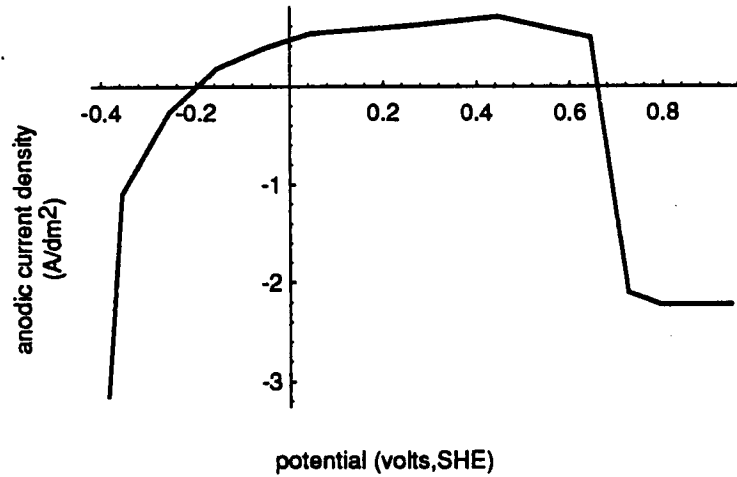


Figure 4-14. Measured anodic current density versus potential for iron in sulfuric acid solution (Valdes, 1987)

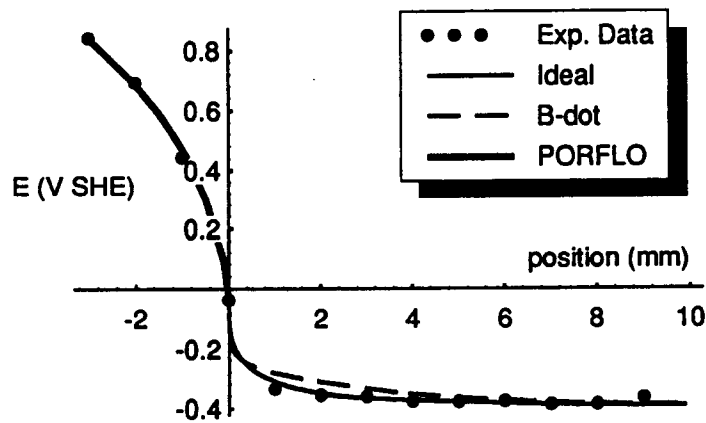


Figure 4-15. Experimental and predicted corrosion potentials with and without complexation for iron in sulfuric acid solution (Valdes, 1987, experiment)

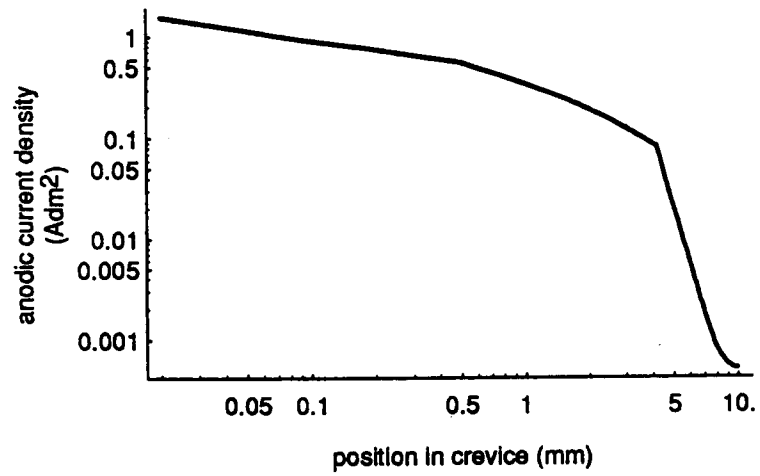


Figure 4-16. Anodic current density at metal/solution interface for iron in sulfuric acid solution (Valdes, 1987, experiment)

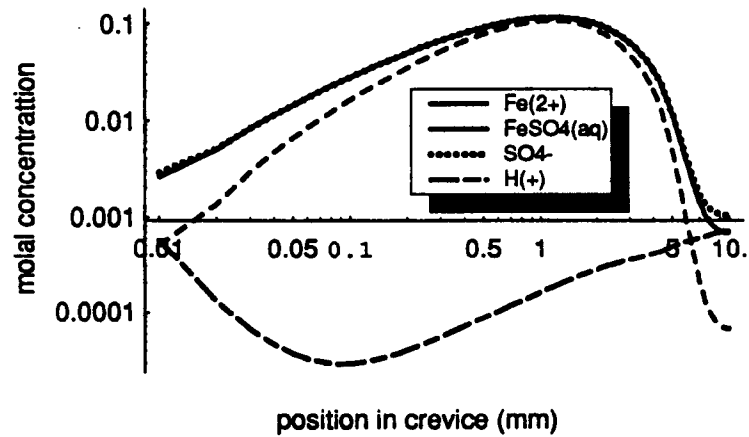


Figure 4-17. Predicted species concentration for iron in sulfuric acid solution

5 CONCLUSION

A reactive transport model optimized for the analysis of crevice corrosion has been developed. The computer code implementing the model is general in format, allowing specification of species and reactions considered at run time. Previously published models for crevice corrosion [Sharland, (1992), Watson, 1989, Watson and Postlewaite, (1990), Walton, (1990)] are either limited to steady state simulations or (for the transient models) limited to the case of a constant anodic current density (passive metal). Additionally, the referenced models all assume dilute solution theory for mass transport. *Twitch* removes many of these limitations, allowing for simulation of transient, active corrosion with full consideration of individual ion activity coefficients in the thermodynamic and mass transport calculations.

Comparison of modeled and experimental data for three different systems with iron and stainless steel gives agreement ranging from approximate (Alavi and Cottis data) to excellent (Valdes data). This likely represents ranges in the complexity of the experimental systems and the completeness of the experimental data set required for modeling the system. A general problem in the corrosion field is that experiments are rarely designed to obtain parameters (e.g., polarization curves from uncreviced specimens) required for modeling.

Major input parameters for the model requiring experimental input are:

- Initial and boundary conditions for all aqueous species, solids, and the potential
- System geometry, especially crevice gap.

Other input parameters, such as diffusion coefficients and thermodynamic data are generally obtained from the literature. In the case of the Alavi and Cottis data, the electrode kinetics were not measured. This limitation required that the current density for the purposes of modeling be assumed. The cleanest and simplest assumption (and the one used in this report) is a constant current density throughout the crevice as might be expected from a passivated metal. The lack of kinetic information for reactions at the metal/solution interface limits the usefulness of this (or any) model in simulating the Alavi and Cottis data since the unknown parameters can be used as calibration or fit factors. The results for the Alavi and Cottis (1987) data suggest that the pH at the crevice base can be reproduced with a model current density of 10^{-4} A/dm² whereas a current density intermediate between 10^{-4} and 10^{-5} A/dm² is required to reproduce measured potential drops. The pH minimum measured near the mouth cannot be reproduced assuming a constant anode current density.

In contrast, the Valdes data for the chemically simpler iron metal, is sufficiently complete to allow simulations based only upon data obtained external from the crevice. The electrode kinetics were obtained from polarization curves drawn on uncreviced specimens, the initial and boundary conditions were based upon initial conditions and boundary potential measured in the experiments, and the crevice geometry was carefully controlled. Transport and thermodynamic data were obtained from the literature. No free or floating parameters were available in the model to improve or adjust the relationship between experimental data and modeling results. This is a very important distinction. The model results for the Valdes experiments with iron crevices in sulfuric acid and acetate electrolytes can be viewed as predictions — and they predict the system very well.

6 REFERENCES

- Alavi, A. and R. A. Cottis, 1987, The Determination of pH, Potential and Chloride Concentration in Corroding Crevices on 304 Stainless Steel and 7475 Aluminium Alloy, *Corrosion Science*, Vol. 27, No. 5, pp. 443-451.
- Bockris, J. O'M, and M.D.N. Reddy, 1977, *Modern Electrochemistry*, Plenum Press, New York.
- Helgeson, H.C., 1969, "Thermodynamics of Hydrothermal Systems at Elevated Temperatures and Pressures," *American Journal of Science*, p. 729-804.
- Hindmarsh, 1983, ODEpack, A Systematized Collection of ODE Solvers, in *Scientific Computing*, R.S. Steplemen *et al.* (eds.), North-Holland, Amsterdam, pp. 55-64.
- Lerman, A., 1979, *Geochemical Processes in Water and Sediment Environments*, Wiley, New York.
- Newman, J.S. 1991, *Electrochemical Systems*, Prentice Hall, Englewood Cliffs, New Jersey.
- Perry, R.H., and C.H. Chilton, 1973, *Chemical Engineers' Handbook*, McGraw-Hill, New York.
- Pickering, H.W., 1989, *Corrosion Science*, 29, 325.
- Press, William H., Brian P. Flannery, Saul A. Teukolsky, and William T. Vetterling, 1986, *Numerical Recipes: The Art of Scientific Computing*, Cambridge University Press, Cambridge.
- Runchal, A. B. Sagar, R. G. Baca, and N. W. Kline, 1985, *PORFLO - A Continuum Model for Fluid Flow, Heat Transfer, and Mass Transport in Porous Media: Model Theory, Numerical Methods, and Computational Tests*. Rockwell Hanford Operations, RHO-BW-CR-150-P.
- Sharland, S.M., A Mathematical Model of the Initiation of Crevice Corrosion in Metals, *Corrosion Science*, Vol. 33, No. 2, pp. 183-201, 1992.
- Sharland, S.M., A Review of the Theoretical Modelling of Crevice and Pitting Corrosion, *Corrosion Science*, Vol. 27, No. 3, pp. 289-323, 1987.
- Stumm, W. and J.J. Morgan, 1981, *Aquatic Chemistry, an Introduction Emphasizing Chemical Equilibria in Natural Waters*, John Wiley and Sons, New York, 1981.
- Valdes, A. and H.W. Pickering, 1987, "IR Drops in the Absence of Gas Constrictions During Crevice Corrosion of Iron," pp. 393-401, in *Advances in Localized Corrosion*, ed. H.S. Isaacs, U. Bertocci, J. Kruger, and S. Simialowska, NACE-9, National Association of Corrosion Engineers, Houston, Texas.
- Valdes-Mouldon, A., 1987, Ph.D. Thesis, The Pennsylvania State University.
- Vitagliano, V., and P.A. Lyons, 1956, "Diffusion in Aqueous Acetic Acid Solutions," *Journal of the American Chemical Society*, v.78, pp. 4538-42.

- Walton, J., 1990, Mathematical Modeling of Mass Transport and Chemical Reaction in Crevice and Pitting Corrosion, *Corrosion Science*, Vol. 30, No. 8/9.
- Walton, J., and S.K Kalandros, 1992, *Mariana - A Simple Chemical Equilibrium Solver*, technical report. CNWRA 90-020
- Watson, M.K., 1989, *Numerical Simulation of Crevice Corrosion*, Ph.D. thesis, Department of Chemical Engineering, University of Saskatchewan.
- Watson, M.K., and J. Postletwaite, 1990, Numerical simulation of crevice corrosion of stainless steel and nickel alloys in chloride solutions. *Corrosion*, v.46, n.7, p.522-530.
- Wolery, T.J., 1983, *EQ3NR A Computer Program for Geochemical Aqueous Speciation Solubility Calculations: User's Guide and Documentation*, UCRL-53414, Livermore, California.
- Wolery, T.J., K.J. Jackson, W.L. Bourcier, C.J. Bruton, B. E. Viani, K. G. Knauss, and J.M. Delany, 1990, *Current Status of the EQ3/6 Software Package for Geochemical Modeling*, in D. C. Melchior and R.L. Bassett, editors, *Chemical Modeling of Aqueous Systems II*, ACS symposium Series 416, American chemical Society, Washington, DC.

APPENDIX A
STRUCTURE OF CODE

STRUCTURE OF CODE

Twitch is written in standard FORTRAN 77 with real*8 variables. Data are read in from an input deck and written to an output file. With the Unix operating system they are specified in the command line as follows:

```
Twitch3 <filename.in > filename.out
```

The main code is contained in the file "*Twitch.f*". Variables are passed between subroutines through four common files, listed below with their contents:

param.f: parameters for dimensioning arrays
eq.f: chemical reaction data for the *Mariana* subroutine
xport.f: variables for mass transport calculations
conc.f: concentration data

The following list summarizes the subroutine hierarchy of *Twitch*. The name of the file containing each subroutine is given in parentheses unless the subroutine resides in the same file as the routine which called it:

- I. Input (*Twitch.f*)
- II. (ode.f or Isodes.f)
 - A. derivs (derivs.f)
 - 1. der (der.f)
 - a). corrode (corrode.f)
 - b). gradient (der.f)
 - 2. derivs (derivs.f)
- III. *Mariana* (Mar.f)
- IV. chempot (der.f)
- V. gradient (der.f)

Mariana calls several subroutines which are contained in the "Mar.f" file. A brief summary of the *Mariana* subroutine is given in Appendix II.

The corrode subroutine may also call subroutines. However, this is dependent upon the individual application, so no subroutines are listed here.

APPENDIX B

SUMMARY OF *MARIANA* SUBROUTINE

SUMMARY OF *MARIANA* SUBROUTINE

The *Mariana* subroutine will not be described in detail here because it is the subject of another report (see Walton and Kalandros, 1992, for a complete explanation). However, a brief summary is in order.

Mariana determines the equilibrium concentrations of each species by minimizing the Gibbs Free Energy change of each reaction (ΔG_r). This is done by setting the first derivative of ΔG_r equal to zero and solving for the extent of each reaction using a Newton-Raphson solver, which is implemented in the *LUDCMP* and *LUBKSB* subroutines. This solver requires a Jacobian matrix, so the *ddfunc* and *dfunc* subroutines are used to determine the second derivative of ΔG_r .

The *DoReact* subroutine reacts the species present according to the stoichiometric matrix provided in the input deck. The *Activity* subroutine calculates the activities of each aqueous species by multiplying its concentration by its activity coefficient, which is calculated by the *Gamma* subroutine.

The following list is a summary of the interaction of these subroutines as it would appear in the *Twitch* subroutine hierarchy in Appendix I:

- III. *Mariana* (Mar.f)
 - A. *Activity*
 - 1. *Gamma*
 - B. *ddfunc*
 - 1. *dfunc*
 - C. *LUDCMP*
 - D. *LUBKSB*
 - E. *DoReact*

APPENDIX C
OPERATING INSTRUCTIONS

OPERATING INSTRUCTIONS

This section describes the input and output conventions of *Twitch*. The Valdes Sulfate model will be used as an example. Data is read into *Twitch* through an input deck.

The first line of the input file contains three numbers:

100,9,5\ number of nodes, number of species, number of reactions

The "\ " specifies that what follows are just comments as opposed to data that *Twitch* might be interested in. As indicated by the comments, the first number specifies the number of nodes in the system, the second specifies the number of species involved, and the third specifies the number of reactions simulated. These values must be included so *Twitch* will know how many lines of data to read from the input deck.

The next section is dedicated to species data:

name(i),	u0,	d,	z,	anodic,bca,	ica,ibca,ibcb,iphase,solve,a0
'H(+)',	0.	.31e-7,	+1.,	0.,	2.e-3, 2.e-3,1,2,1,1,9.0
'OH(-)',	-157293.,	5.00e-7,	-1.,	0.,	1.e-10, 1.e-10,1,2,1,1,3.0
'H2O',	-237178.,	0.,	0.,	0.,	10.0, 10.0,1,2,4,0,3.0
'Fe(2+)',	-78870.,	0.71e-7,	+2.,	1.,	1.e-10, 1.e-10,1,2,1,1,6.0
'SO4(2-)',	-744630.,	1.1e-7,	-2.,	0.,	1.e-3, 1.e-3,1,2,1,1,4.0
'Fe(OH)(+)',	-277400.,	1.0e-7,	+1.,	0.,	1.e-10, 1.e-10,1,2,1,1,4.0
'FeSO4(aq)',	-848520.,	0.77e-7,	0.,	0.,	1.e-10, 1.e-10,1,2,1,1,3.0
'FeSO4(s)',	-820800.,	0.,	0.,	0.,	0.,1,2,2,0,0.0
'FeSO4:7H2O(s)',	-2510270.,	0.,	0.,	0.,	0.,1,2,2,0,0.0

The second line overall is a required comment line which *Twitch* skips when reading in data. This line allows the user to make a note of what each column represents. Data input is unformatted and all columns must be set off by commas; whitespace characters (space and tab) are ignored. *Twitch* uses the *nspecies* number above to determine how many lines of data to read in.

The first column is the name of the species. The character string for each species must be enclosed in single quotes. What is actually inside the quotes is irrelevant to *Twitch*; the code uses these character strings to identify species in the output file.

The second column represents the standard Gibbs Free Energy of the species, otherwise known as its standard state chemical potential, in joules per mole. This is required by *Mariana* in order to equilibrate the system (Walton and Kalandros, 1992).

The third column is the diffusion coefficient of the species, given in decimeters squared per second ($\text{dm}^2 \text{s}^{-1}$). In this example, water and solids were given coefficients of "0" because they were assumed not to diffuse. Other time units besides seconds may be used as long as consistency is maintained in the input data.

The fourth column is the charge of the species

The fifth column is the fraction of the anodic current density consisting of a particular species. In this example, iron is the only species being corroded, so the anodic current density is 100% iron. Note that the values of this column should add up to 1.

The sixth column is the boundary condition molal concentrations of the species at the mouth of the crevice. *Twitch* first equilibrates these conditions through a call to *Mariana* and then uses these values as the fixed boundary concentrations at the mouth. Aqueous species with a boundary concentration of zero should be given an extremely small "fictitious concentration" such as 10^{-20} ; entering a "0" here will cause an error because of logarithmic calculations. The concentration of water is unimportant as long as it is present in excess. In this example, the solution is 0.001 molal H_2SO_4 , so the concentrations of H^+ and SO_4^{-2} are 2×10^{-3} and 1×10^{-3} , respectively.

The seventh column is the initial concentration in the crevice. Generally, the values in this column should be equal to those in the previous column. The eighth and ninth columns indicate the type of boundary condition, with a "1" indicating a constant concentration and a "2" indicating a no-flux boundary.

The tenth column indicates the phase of the species: "1" for aqueous, "2" for solid, "3" for gas, and "4" for water. The present version of *Twitch* cannot account for gaseous species.

The next column is a flag for whether or not the mass transport part of the code should solve for that particular species. Normally, aqueous species are given a "1" here, indicating that their transport equations will be solved, while solid species are given a "0" to indicate that their transport equations will not be solved.

The final column is the A-zero value of the species, which is a constant used in *Mariana* to calculate activity coefficients. This value is only important if the B-dot equation is selected for the determination of activity coefficients.

The next section of the input file contains the stoichiometric matrix:

```
1., 0., 0., 0., 1.\ H(+)  rows = species, columns = reactions
1., 0., 0., 0., 0.\ OH(-)  products (+) reactants (-)
-1., 0., 0., -7., -1.\ H2O
0., -1., -1., -1., -1.\ Ferrous Iron
0., -1., -1., -1., 0.\ SO4(2-)
0., 0., 0., 0., 1.\ Fe(OH)(+)
0., 1., 0., 0., 0.\ FeSO4(aq)
0., 0., 1., 0., 0.\ FeSO4(s)
0., 0., 0., 1., 0.\ FeSO4:7H2O(s)
```

The rows indicate participation of each species in the different reactions, which are indicated by the columns. Again, *Twitch* uses the *nspecies* number to determine how many lines of data to read in from this section. The values listed are equal to the stoichiometric coefficients of the species in the reactions described. A negative value indicates that the species is a reactant while a positive value indicates that the species is a product. For instance, the first column indicates the disassociation of water:



The next section describes the division of the crevice into nodes:

```
0.000, 0.0001, 0.0002, 0.0003, 0.0004, 0.0005, 0.0006, 0.00075, 0.0009, 0.0011 \ 100 nodal locations
0.0014, 0.0018, 0.0023, 0.003, 0.004, 0.005, 0.006, 0.007, 0.008, 0.009
0.010, 0.011, 0.012, 0.013, 0.014, 0.015, 0.016, 0.017, 0.018, 0.019
0.020, 0.021, 0.022, 0.023, 0.024, 0.025, 0.026, 0.027, 0.028, 0.029
0.030, 0.031, 0.032, 0.033, 0.034, 0.035, 0.036, 0.037, 0.038, 0.039
0.040, 0.041, 0.042, 0.043, 0.044, 0.045, 0.046, 0.047, 0.048, 0.049
0.050, 0.051, 0.052, 0.053, 0.054, 0.055, 0.056, 0.057, 0.058, 0.059
0.060, 0.061, 0.062, 0.063, 0.064, 0.065, 0.066, 0.067, 0.068, 0.069
0.070, 0.071, 0.072, 0.073, 0.074, 0.075, 0.076, 0.0775, .079, 0.081
0.083, 0.085, 0.087, 0.089, 0.092, 0.095, 0.097, 0.099, 0.0995, 0.1005
```

Although the crevice itself is considered to be one-dimensional, the node positions are given in ten rows of ten values. The values indicate distance into the crevice in decimeters (dm). The first value should be zero, indicating the mouth itself. In the present version of the code, the last value is used to determine where the no-flux boundary is. The boundary is located halfway between the last two nodes; thus, the last value listed should be a mirror of the previous value. In this example, the last value is 0.1005 dm = 1.005 cm to mirror the previous value, 0.995 cm, across the boundary at 1.000 cm.

A maximum of 100 values may presently be entered; the user can expand this through appropriate modifications to the "param.f" file (Walton and Kalandros, 1992) and the *Input* subroutine. If less than the maximum number of nodes is entered, the remaining values must be filled with numbers, preferably zero filled; *Twitch* always reads ten rows of ten values from this section.

Normally, most of the action involved in crevice corrosion occurs around the mouth of the crevice; thus, the user should provide *Twitch* with a finer grid around the mouth and a coarser grid for the rest of the crevice.

The next two lines list the values of various constants and flags:

```
5.0e-3, 298.15, 8.314, 96500., 1.e-0, 1 \ gap, temp, Rgas, Faraday const, i passive, igamma flag
5, 0.036, 1.e-4, 1, 0.5 \ # solve cards, boundary potential, eps, ODE solver flag, relax
```

The first value in the first line is the width of the crevice or gap in decimeters (dm). The second value is the absolute temperature in Kelvin, the third is the value of the ideal gas constant in joules per mole per degree Kelvin, and the fourth is the value of the Faraday constant in joules per volt-equivalent. The next number is the value of the anodic current density in amps per decimeter squared (A dm^{-2}). The default version of the code assumes a constant anodic current density equal to this value. This number has no meaning for modifications involving active corrosion. The final value in the first line is the activity coefficient calculation flag, which is used by *Mariana* to determine how to calculate activity coefficients. If this value is "0", then the ideal case is assumed, and all activity coefficients are set equal to 1. If this value is "1", the B-dot equation is used to calculate the coefficients; if this value is "2", the Davies equation is used.

The first number in the second line is the number of solve commands. The user may specify the size of the time step and the number of steps used for each solve card as described below. Note that the role of the time step variable is limited because all of the ODE integrators used have variable time steps for error control; the value specified dictates how often the code switches between the equilibration step and the mass transport step. *Twitch* prints out results at the end of each solve card as described later.

The second value in this line is the boundary condition for the potential in solution (ϕ_s), or the potential in solution at the crevice mouth, in volts (SHE). This value is meaningless for the default version of the code but is useful for customized *corrode* subroutines. The third value is the tolerance for the ODE solvers and the fourth value is the ODE solver flag. A "0" indicates the Adams method (Hindmarsh, 1983); a "1" indicates the Bulirsch-Stoer method (Press, *et al*, 1986); and a "2" indicates the 5th-order Runge-Kutta method. The fifth value is the relaxation factor for the calculation of the potential in solution.

The remaining lines of the code give the size of the time step in seconds and number of time steps for the different solve cards:

```
0.0001, 10
0.1, 50
0.25, 2400 ! 10 minutes
0.25, 2400 ! 10 minutes
0.25, 2400 ! 10 minutes
```

Since five time cards were specified in the preceding line, five solve card lines are given here. The first card, for example, prints the output data after taking ten steps of 0.0001 seconds. These first two solve cards are mainly intended to improve prediction of the values of the potential in solution; for this particular experiment, *Twitch* was used to model active crevice corrosion, so smaller time steps were required for *Twitch* to predict the transition from passive to active corrosion. The solve cards are followed sequentially; thus, the remaining three solve cards instruct *Twitch* to print the results every ten minutes for the next half hour.

Now that the input deck has been created, *Twitch* can be invoked with the command line (Unix operating system):

```
Twitch3 <filename.in >filename.out
```

where *filename.in* is the name of the input deck and *filename.out* is the name of the output file. Omission of the output filename causes the output to be printed to the screen.

Twitch first writes data to the output file as it reads it from the input deck; thus, all the data from the input deck is echoed in the output file. *Twitch* then prints out the following data after every solve card: species data at each node; potential in solution data at each node; a charge balance at each node; and current in solution data at each node. There are no data for the last node entered because it is a dummy node as described above. The data in each section is arranged in columns with the first column being the distance into the crevice; each row represents, therefore, the data at a specific node. *Twitch* includes comment lines to identify each section. For the species data, the second column is the molal concentration of the species, the third is the activity coefficient of the species, and the fourth is the chemical potential of the species. For the potential in solution, the second column is the potential in solution in volts (SHE), the third is the rate of change of the potential or potential gradient, and the fourth is the current density at the metal/solution interface in amps per decimeter squared. For the charge balance, there are only two columns, with the second column being the result of Eq. (2-6) in coulombs. This is intended as an error-checking output; the values in the second column should be extremely small to indicate that the code is actually preserving electroneutrality. For the current in solution, the second column is the result of Eq. (2-7) in amps per decimeter squared, the third is the value of Eq. (2-3), and the fourth is the current density at the metal/solution interface as above. Again, the second and third columns are mainly an error checking output; the values in the second column should be about equal to the values in the third column.

In addition to creating *filename.out*, *Twitch* also creates two other files, "key" and "plot". The "plot" file contains the concentration, potential in solution, current in solution, and current density at the metal solution interface data at each node at the end of each time plane; only the first and second columns of the data written to the output file are recorded in "plot". The data is arranged in a way such that the user may easily extract the data from the file. Unlike *filename.out*, "plot" contains no labels to identify the data listed. Instead, following each line of data is a third column which contains an identification number; this number specifies either the name of the species or potential or current in solution as well as the time at which the data was printed. The "key" file describes what each number represents. The following is an extract from the Sulfate model "key" file:

```
H(+) at time 605.00100000000 key 24
OH(-) at time 605.00100000000 key 25
H2O at time 605.00100000000 key 26
Fe(2+) at time 605.00100000000 key 27
SO4(2-) at time 605.00100000000 key 28
Fe(OH)(+) at time 605.00100000000 key 29
FeSO4(aq) at time 605.00100000000 key 30
FeSO4(s) at time 605.00100000000 key 31
FeSO4:7H2O(s) at time 605.00100000000 key 32
Potential at time 605.00100000000 key 33
Current at time 605.00100000000 key 34
Anodic Current at time 605.00100000000 key 35
```

This identification scheme allows the user to extract data from the "plot" file using the following UNIX command:

```
grep 'key' plot
```

Here, key is the identification number from the "key" file. As an example, the following command will extract the concentration data for the Fe^{2+} ion at time 605 (a little over 10 minutes) and write it to a file called "ron.ion"

```
grep '27' plot > iron.ion
```

The "grep" command searches the file specified (in this case, "plot") for the desired string (in this case, "27") and prints any line of text containing that string. Thus, for the example listed above, the file "iron.ion" would contain the following lines:

```
0.00000E+00 1.87464E-07 27
1.00000E-04 2.53941E-04 27
2.00000E-04 4.37611E-04 27
3.00000E-04 5.60328E-04 27
4.00000E-04 6.46253E-04 27
5.00000E-04 7.10200E-04 27
6.00000E-04 7.60589E-04 27
7.50000E-04 8.20282E-04 27
9.00000E-04 8.67383E-04 27
1.10000E-03 9.16534E-04 27
1.40000E-03 9.68828E-04 27
```


.....
9.70000E-02 9.44494E-06 27
9.90000E-029.42881E-06 27
9.95000E-029.42730E-06 27

All output files are standard ASCII files which may be read into other software for analysis.